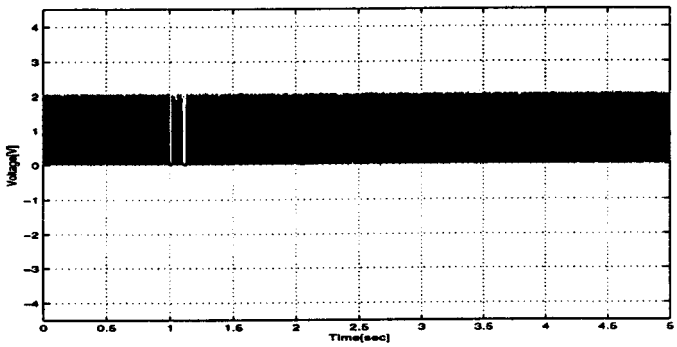


Fig. 31. Control voltage of the sliding-mode controller without an integrator.

## VIII. Conclusions

This paper has presented a method to control the angular displacement of a magnetically suspended balance beam with plant parametric variations and external disturbances. To overcome the effect of the parametric variations, and to reject the external disturbance forces, we used an integral sliding-mode controller. We derived the mathematical model of the balance beam, including an integral compensator, then we designed the linear and nonlinear control components. We showed the insensitivity of the controller response under the parametric variations and the disturbance rejection by simulations. Finally, we proved the effectiveness of the integral sliding-mode controller by experimentation. Extensions of this work to other bearing systems, such as an artificial heart pump, which employs the electromagnetic bearings, and to other uncertainties and disturbance such as sinusoidal are currently under investigation.

## References

[1] P. E. Allaire and A. Sinha, "Robust sliding mode control of a planar rigid rotor system on magnetic bearings," presented at the Proc. 6th Int. Symp. Magnetic Bearings, Cambridge, MA, Aug. 5–7, 1998, pp. 577–586.

[2] S. Ueno, J. H. Lee, P. E. Allaire, and Y. Okada, "Sliding mode control of magnetic bearings: Comparison of sensed and self sensing performance," in *Proc. ASME*, Indianapolis, IN, June 7–10, 1999.

[3] C. Edwards and S. K. Spurgeon, *Sliding Mode Control-Theory and Application*. New York: Taylor & Francis, 1998.

[4] K. Nonami and K. Den, *Sliding Mode Control-Design Theory of Nonlinear Robust Control (Japanese Version)*. Tokyo, Japan: Corona Publishing, 1994.

[5] S. K. Spurgeon and R. Davies, "A nonlinear control strategy for robust sliding mode performance in the presence of unmatched uncertainty," *Int. J. Control*, vol. 57, no. 5, pp. 1107–1123, 1993.

[6] T. L. Chen and Y. C. Wu, "Integral variable structure control approach for robot manipulators," in *Proc. Inst. Elect. Eng.*, vol. 138, Mar. 1992, pp. 161–166.

[7] ——, "Design of integral variable structure controller and application to electrohydraulic velocity servosystems," in *Proc. Inst. Elect. Eng.*, vol. 138, Sept. 1991, pp. 439–444.

[8] E. Hilton, M. Humphrey, V. Stankovic, and P. Allaire, "Real time control of a magnetic bearing suspension system for flexible rotors," in *Proc. 5th Int. Symp. Magnetic Suspension Technology*, Santa Barbara, CA, Dec. 1–3, 1999, pp. 443–457.

# Model-Free Regulation of Multilink Smart Materials Robots

S. S. Ge, T. H. Lee, and Z. P. Wang

***Abstract*—In this paper, model-free controllers for multilink smart materials robots are presented. The approach allows controller design in the absence of a system model which is complex and difficult to obtain for multilink smart materials robots, and provides additional degrees of freedom in feedback control design. Simulation results are provided to show the effectiveness of the presented approach.**

***Index Terms*—Model-free control, multilink, smart materials robots.**

## I. Introduction

In recent years, with the promised advent of lightweight high strength composite materials, much attention has been given to modeling and control of flexible-link manipulators. The flexible-link robot is governed by a set of partial differential equations, which means that the system is of infinite dimensionality. However, the majority of the research effort has been on control of the end effector through actuation by the joint motors in the literature. Based on a truncated (finite dimensional) model obtained from either the finite element method (FEM) or assumed modes method (AMM), various kinds of control approaches have been applied to improve the performance of flexible systems [1]–[5]. To avoid the problems associated with the truncated model, such as controller/observer spillover problems [6], some controllers are designed based on the partial differential equations (PDEs) directly [6]–[8]. While most research is dealing with the single flexible-link case for its simplicity, some work for multilink flexible-link robots have also been studied [5], [9].

Recently, utilization of smart or intelligent materials in the control of flexible structures is receiving increased attention [10]–[13]. In this paper, by combining the results in [9] for multilink flexible robots and those in [13] for single-link smart materials robots, decentralized and centralized model-free controllers for multilink smart materials robots are presented. The controllers are developed based on the basic energy–work relationship, and subsequently avoid the problems associated with model-based methods. The controllers are very robust in terms of system parameter variations and can guarantee the stability of the closed-loop system. In addition, by using a simple adaptive gain tuning method, an adaptive centralized model-free controller is presented for satisfactory performance and ease of implementation.

## II. Multilink Smart Materials Robot

We shall consider an $N$-link smart materials robot interconnected by $N$ motors as shown in Fig. 1. The system can be either deployed in space or configured in the horizontal plane. In both cases, the effects of gravity are neglected.

Let $\theta_{di}$ denote the desired joint angular position for link $i$, while $\theta_i$ is the actual joint angle, $\tau_i$ is the torque applied to the joint. Assuming $n_i$ pairs of piezoelectric sensors and actuators collocated at $n_i$ points along link $i$, $\mathbf{v}_i = [v_{i1}\ v_{i2}\ \ldots\ v_{in_i}]^T \in R^{n_i}$ is the vector of control voltages applied to actuators, while $\mathbf{I}_i = [I_{i1}\ I_{i2}\ \ldots\ I_{in_i}]^T \in R^{n_i}$ is

Manuscript received November 11, 2000; revised May 10, 2001. Recommended by Technical Editor M. Meng.

The authors are with the Department of Electrical and Computer Engineering, National University of Singapore, Singapore 117576 (e-mail: elegesz@nus.edu.sg).

Publisher Item Identifier S 1083-4435(01)08152-2.

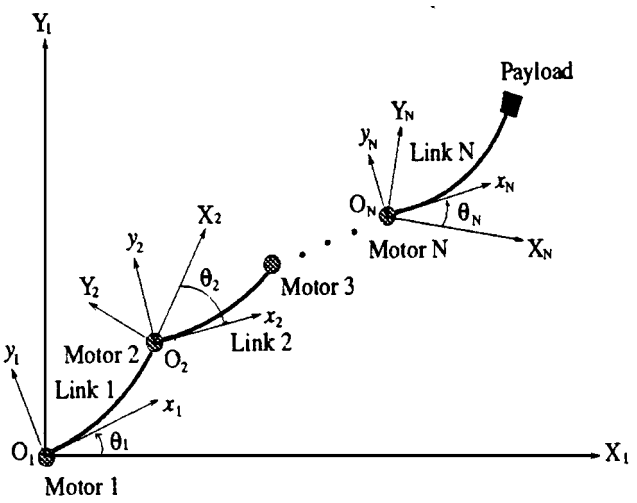


Fig. 1. Geometry of an $N$-link smart materials robot.

the vector of the electrical currents induced by sensors, $I_{ij}$ is proportional to the change of strain [14].

Hence, the total work done by external inputs $W = \sum_{i=1}^{N}\int_0^t \tau_i(t)\dot{\theta}_i(t)dt + \sum_{i=1}^{N}\int_0^t \mathbf{v}_i^T\mathbf{I}_i dt$, which consists of that done by the torque applied to the $N$ joints and that contributed by the voltages applied to piezoelectric actuators. Damping and friction are neglected because their exclusion will not affect the closed-loop stability. Thus, from the energy–work relationship, we have the following equation:

$$[E_k(t)+E_p(t)]-[E_k(0)+E_p(0)] = \sum_{i=1}^{N}\int_0^t \dot{\theta}_i(t)\tau_i(t)dt + \sum_{i=1}^{N}\int_0^t \mathbf{I}_i^T\mathbf{v}_i dt \tag{1}$$

where $E_k(t)$ and $E_k(0)$, $E_p(t)$ and $E_p(0)$ are the total kinetic energy and total potential energy of system at time $t$ and 0, respectively. Then, we have

$$\dot{E}_k(t)+\dot{E}_p(t) = \sum_{i=1}^{N}\dot{\theta}_i(t)\tau_i(t) + \sum_{i=1}^{N}\mathbf{I}_i^T\mathbf{v}_i. \tag{2}$$

## III. Model-Free Controller Design

In this section, two kinds of model-free controllers are presented for multilink smart materials robots. The control objective here is to rotate each link of the robot to the desired angular position and simultaneously suppress the residual vibrations effectively. Although the traditional joint proportional and differential (PD) controller can stabilize the flexible robots, the system performance is not good because there are no explicit efforts introduced to suppress the residual vibrations. Better control performance is expected by appropriately exploiting the additional control capability available.

### A. Decentralized Model-Free Controller (DMFC)

In certain cases, decentralized controllers are very desirable because of the technical difficulties in implementing communications among the controllers located at different places; and the inherent robustness of a decentralized control system.

Consider the following DMFC:

$$\mathbf{u}_i = \begin{bmatrix}\tau_i \\ \mathbf{v}_i\end{bmatrix} = \begin{bmatrix}-k_{pi}[\theta_i(t)-\theta_{di}]-k_{vi}\dot{\theta}_i(t) \\ -\mathbf{K}_{psi}\int_0^t \mathbf{I}_i dt - \mathbf{K}_{vsi}\mathbf{I}_i\end{bmatrix} \tag{3}$$

where $\mathbf{K}_{psi} = \mathrm{diag}[k_{psi_k}] \in R^{n_i\times n_i}$, $\mathbf{K}_{vsi} = \mathrm{diag}[k_{vsi_k}] \in R^{n_i\times n_i}$, and $k_{pi}$, $k_{vi}$, $k_{vsi_k} > 0$, $k_{psi_k} \geq 0$, $i = 1, 2, \ldots N$.

*Theorem 1:* The closed-loop multilink smart materials robot system is stable if the control inputs are given by (3).

*Proof:* Consider the following Lyapunov function candidate:

$$V_1(t) = E_k(t)+E_p(t)+\frac{1}{2}\sum_{i=1}^{N}k_{pi}[\theta_i(t)-\theta_{di}]^2 + \frac{1}{2}\sum_{i=1}^{N}\left(\int_0^t \mathbf{I}_i dt\right)^T\mathbf{K}_{psi}\left(\int_0^t \mathbf{I}_i dt\right). \tag{4}$$

It is a Lyapunov function candidate because the energy of system $E_k(t)+E_p(t) \geq 0$.

By virtue of (2) and (3), the time derivative of $V_1$ is given by

$$\dot{V}_1(t) = -\sum_{i=1}^{N}k_{vi}\dot{\theta}_i(t)^2 - \sum_{i=1}^{N}\mathbf{I}_i^T\mathbf{K}_{vsi}\mathbf{I}_i \leq 0$$

thus, the closed-loop system is energy dissipative and, hence, stable.

### B. Centralized Model-Free Controller (CMFC)

In order to further improve the control performance and consider those situations that centralized controllers can be implemented, we shall study the CMFC design.

Consider the following CMFC:

$$\mathbf{u_i} = \begin{bmatrix}\tau_i \\ \mathbf{v}_i\end{bmatrix} = \begin{bmatrix}-k_{pi}[\theta_i(t)-\theta_{di}]-k_{vi}\dot{\theta}_i(t)-\tau_{ci} \\ -\mathbf{K}_{psi}\int_0^t \mathbf{I}_i dt - \mathbf{K}_{vsi}\mathbf{I}_i - \mathbf{v}_{ci}\end{bmatrix} \tag{5}$$

where $\tau_{ci} = \sum_{j=1}^{m_0}k_{\theta j}f_{\theta j}(t)\int_0^t \dot{\theta}_i(s)f_{\theta j}(s)ds$, and $\mathbf{v}_{ci}$ is a column vector defined as

$$\mathbf{v}_{ci} = \begin{bmatrix}\sum_{j=1}^{m_1}k_{1j}f_{1j}(t)\int_0^t I_{i1}(s)f_{1j}(s)ds \\ \sum_{j=1}^{m_2}k_{2j}f_{2j}(t)\int_0^t I_{i2}(s)f_{2j}(s)ds \\ \vdots \\ \sum_{j=1}^{m_{n_i}}k_{n_ij}f_{n_ij}(t)\int_0^t I_{in_i}(s)f_{n_ij}(s)ds\end{bmatrix} \in R^{n_i}.$$

$f_{\theta j}$, $f_{kj}$s are any time-integrable signals, $\mathbf{K}_{psi} = \mathrm{diag}[k_{psi_k}] \in R^{n_i\times n_i}$, $\mathbf{K}_{vsi} = \mathrm{diag}[k_{vsi_k}] \in R^{n_i\times n_i}$, $k_{pi}$, $k_{vi}$, $k_{vsi_k} > 0$, $k_{psi_k} \geq 0$, and $k_{\theta j}$, $k_{kj} \geq 0$.

*Theorem 2:* The closed-loop multilink smart materials robot system is stable if the control inputs are given by (5).

*Proof:* Consider the following Lyapunov function candidate:

$$V_2(t) = V_1(t)+\frac{1}{2}\sum_{i=1}^{N}\sum_{j=1}^{m_0}k_{\theta j}\left[\int_0^t \dot{\theta}_i(s)f_{\theta j}(s)ds\right]^2 + \frac{1}{2}\sum_{i=1}^{N}\sum_{k=1}^{n_i}\sum_{j=1}^{m_k}k_{kj}\left[\int_0^t I_{ik}(s)f_{kj}(s)ds\right]^2 \tag{6}$$

where $V_1(t)$ is defined in (4).

Taking the time derivative of $V_2$ and applying (2) and (5), we arrive at

$$\dot{V}_2(t) = -\sum_{i=1}^{N}k_{vi}\dot{\theta}_i(t)^2 - \sum_{i=1}^{N}\sum_{k=1}^{n_i}k_{vsi_k}I_{ik}^2(t) \leq 0$$

which means that the closed-loop system is stable.

In CMFC, explicit evaluation of deflection related variables provides direct control efforts on vibration suppression. However, it is not easy to find suitable gains of the terms for a satisfactory control performance. In order to improve the performance of proposed CMFC controller, it is desirable to tune the feedback gain of $\tau_{ci}$ and $\mathbf{v}_{ci}$, rather than keep them constants. Unlike the well-known model-based adaptive control where it is required to estimate the physical parameters of the plant and

then tune parameters of the controller adaptively, a simple adaptive gain tuning method is proposed for ease of implementation here.

Let $k_{\theta j} = Y_{\theta j}^2$ and $k_{kj} = Y_{kj}^2$, the adaptation laws are given by

$$\dot{Y}_{\theta j}(t) = \alpha_{\theta j} Y_{\theta j} \dot{\theta}_i f_{\theta j}(t) \int_0^t \dot{\theta}_i f_{\theta j}(s) ds - \sigma_{\theta j} Y_{\theta j}(t) \tag{7}$$

$$\dot{Y}_{kj}(t) = \alpha_{kj} Y_{kj} I_{ik} f_{kj}(t) \int_0^t I_{ik} f_{kj}(s) ds - \sigma_{kj} Y_{kj}(t) \tag{8}$$

where $\alpha_{\theta j} > 0$, $j = 1, \ldots, m_0$, $\alpha_{kj} > 0$, $j = 1, \ldots, m_k$, $k = 1, \ldots, n_i$, and $i = 1, \ldots, N$. The *$\sigma$-terms* in (7) and (8) are introduced to avoid divergence of the integral gains in the presence of disturbances.

*Theorem 3:* The proposed control law (5) with the adaptation laws (7) and (8) can guarantee the stability of the closed-loop multilink smart materials robot system.

*Proof:* Consider the following Lyapunov function candidate:

$$\begin{aligned} V_3(t) =& E_k(t) + E_p(t) + \frac{1}{2} \sum_{i=1}^{N} k_{pi} [\theta_i(t) - \theta_{di}]^2 \\ &+ \frac{1}{2} \sum_{i=1}^{N} \sum_{j=1}^{m_0} \alpha_{\theta j}^{-1} Y_{\theta j}^2 + \frac{1}{2} \sum_{i=1}^{N} \left( \int_0^t \mathbf{I}_i dt \right)^T \\ &\times \mathbf{K}_{psi} \left( \int_0^t \mathbf{I}_i dt \right) + \frac{1}{2} \sum_{i=1}^{N} \sum_{k=1}^{n_i} \sum_{j=1}^{m_k} \alpha_{kj}^{-1} Y_{kj}^2. \end{aligned} \tag{9}$$

Taking the time derivative of $V_3$ and applying (2), (5), (7), and (8), we arrive at

$$\begin{aligned} \dot{V}_3(t) =& -\sum_{i=1}^{N} k_{vi} \dot{\theta}_i^2(t) - \sum_{i=1}^{N} \sum_{j=1}^{m_0} \alpha_{\theta j}^{-1} \sigma_{\theta j} Y_{\theta j}^2 \\ &- \sum_{i=1}^{N} \sum_{k=1}^{n_i} k_{vsi_k} I_{ik}^2(t) - \sum_{i=1}^{N} \sum_{k=1}^{n_i} \sum_{j=1}^{m_k} \alpha_{kj}^{-1} \sigma_{kj} Y_{kj}^2 \leq 0 \end{aligned}$$

which means that the closed-loop system is stable.

*Remark 1:* There are no restrictions on the choices of $f_{\theta j}$ and $f_{kj}$, they can be any variable related to the vibration of the links, or any combination of the bending variables. Theoretically, the stability of the system will not be affected for any time integrable functions $f_{\theta j}$, $f_{kj}$, but it is preferable to select them be associated with the vibration of the flexible link.

*Remark 2:* All the controllers (3) and (5), with/without adaptive laws (7) and (8) are independent of system parameters and thus possess stability robustness to system parameters uncertainties. As a matter of fact, the closed-loop system is stable as long as $k_{pi}$, $k_{vi} > 0$, $k_{\theta j}$, $k_{psi_k} \geq 0$, $k_{vsi_k} > 0$, and $k_{kj} \geq 0$. The stability proof is independent of the system dynamics and thus the drawbacks/problems associated with model-based controllers mentioned in Section I are avoided.

*Remark 3:* All the controllers are very easy to implement in practice. The joint position $\theta_i$ and the joint velocity $\dot{\theta}_i$ can be obtained by rotary encoder and tachometer attached to the rotor of motor $i$. $f_{kj}(t)$ and $f_{\theta j}(t)$ can be chosen as any variable or any combination of variables related to the vibration of the links. For example, in the torque control of link 1, $f_{\theta 1}(t)$ can be signals from the second link.

*Remark 4:* In Theorems 1–3, we only claim the closed-loop stability of the system. To prove the asymptotic stability of the system is not easy due to the infinite dimensionality of the system. In the following, instead of giving rigorous proof, we shall show that practically the smart materials robot can only possibly stop at $\theta_i = \theta_{di}$ $(i = 1, 2, \ldots, N)$ without vibrating. Assuming that the $N$ links stop at the position $\theta_i \equiv \alpha_i$ (hence $\dot{\theta}_i \equiv 0$ for $i = 1, 2, \ldots, N$) with $\alpha_i \neq \theta_{di}$. Due to the existence of internal structural damping in a smart materials robot in practice (structural damping is neglected in the proof of Theorems 1–3), the links must tend to stop vibrating and finally be static at the undeformed position. Recalling that $I_{ij}$ is proportional to the change of strain, we have $\mathbf{I}_i = \mathbf{0}$. Hence, there is no energy input to the system since $\dot{\theta}_i \tau_i + \mathbf{I}_i^T \mathbf{v}_i = 0$ and the robot under study is in the horizontal plane. Furthermore, $\int_0^t I_{ij} dt$ is proportional to the strain, $\int_0^t \mathbf{I}_i dt = \mathbf{0}$ when the link is undeformed. As signals $f_{kj}$, $f_{\theta j}$ are chosen to be zero when the link is at rest, because these functions are associated with the vibrations of the link. Consequently, the first term in $\tau_i$ is a nonzero constant, the middle term is zero, and the last term approaches zero (note that $f_{\theta j}(t)$ are zero when the link $i$ is not deformed) and $\mathbf{v}_i = \mathbf{0}$. Therefore, $\tau_i$ approaches a nonzero constant and thus $\theta_i \equiv \alpha_i$ cannot hold. The only possibility is that the flexible link is at the final position $\theta_i \equiv \theta_{di}$ without vibrating, which implies the tip regulation can be practically achieved.

If the system is of finite dimensions, then LaSalle's theorem can be used to prove the asymptotic stability.

*Theorem 4:* Controller (3) can guarantee the asymptotic stability of the damped truncated system where the flexible deflection is described by arbitrarily any finite number of flexible modes. Furthermore, controller (5) with/without adaptive laws (7) and (8) can also guarantee the asymptotic stability of the same truncated system if $f_{kj}$, $f_{\theta j}$ are selected as the functions that are equal to zeros when the smart materials robot is undeformed.

*Proof:* Using the same Lyapunov functions (4), (6), and (9), we consider the motion of the system in the largest invariant set in the set $\dot{V}_i = 0$ $(i = 1, 2, 3)$. In all cases, we have $\dot{\theta}_i \equiv 0$ and $\mathbf{I}_i \equiv \mathbf{0}$. Hence, there is no energy input to the system since $\dot{\theta}_i \tau_i + \mathbf{I}_i^T \mathbf{v}_i = 0$. Subsequently, $\ddot{\theta}_i = 0$, $\tau_i = -k_{pi}(\theta_i - \theta_{di})$, $\mathbf{v}_i = \mathbf{0}$, $i = 1, 2, \ldots, N$.

Firstly, consider link 1. With the aid of Hamilton's principle, considering the motion of system in $\dot{V}_i = 0$ $(i = 1, 2, 3)$, we have the following PDEs of link 1:

$$c_{e1} w_1''(0,t) - k_{p1}(\theta_1 - \theta_{d1}) = 0 \tag{10}$$

$$\rho_{L1} \ddot{w}_1(x_1,t) = -c_{e1} w_1''''(x_1,t), \quad 0 \leq x_1 \leq L_1 \tag{11}$$

and boundary conditions (BCs) of link 1

$$w_1(0,t) = 0 \quad w_1'(0,t) = 0 \tag{12}$$

$$w_1''(0,t) = \frac{k_{p1}}{c_{e1}} (\theta_1 - \theta_{d1}). \tag{13}$$

Because $\dot{\theta}_i \equiv 0$, the robot is operated as if all the motors are locked. Consequently, each motor can be taken simply as a concentrated mass. Hence, the bending moment at the tip of link $i-1$ should be equal to the base bending moment of link $i$, i.e.,

$$c_{e,i-1} w_{i-1}'(L_{i-1},t) = c_{ei} w_i''(0,t), \qquad i = 2, 3, \ldots, N.$$

Considering links 1 and 2, and noting that

$$c_{e2} w_2''(0,t) = -\tau_2 = k_{p2}(\theta_2 - \theta_{d2})$$

thus, we have another boundary condition

$$w_1''(L_1,t) = \frac{k_{p2}}{c_{e1}} (\theta_2 - \theta_{d2}). \tag{14}$$

It is noted that the left-hand sides of (13) and (14) are functions of time, while the right-hand sides are constants. Let us firstly assume that the two constants are zero. It is shown later that either constants being nonzero leads to invalid solutions. Now (13) and (14) can be rewritten as

$$w_1''(0,t) = 0 \quad w_1''(L_1,t) = 0. \tag{15}$$

Using the Method of Separating Variables and the Superposition Principle [15], a solution $w(x,t)$ can be given by

$$w(x_1,t)=\sum_{i=1}^{\infty}\psi_i(x_1)q_i(t) \tag{16}$$

where $\psi_i$ are mode shape functions and

$$q_i(t)=D_2^i e^{\omega_i t}+D_2^i e^{-\omega_i t} \tag{17}$$

where $D_1^i$ and $D_2^i$ are related to the initial conditions of $y_1(x_1,t)$. Note that the "initial" moment $t_0$ should denote the moment when the system motion enters the invariant set, rather than the initial operating moment since we are considering the motion of the system in the largest invariant set in the set $\dot{V}_i=0\ (i=1,2,3)$. $\omega_i$ can be either positive or negative, without loss of generality, let $\omega_i\geq 0$. This leads to $D_1^i=0$ as follows. If $D_1^i\neq 0$, then $\lim_{t\to\infty}q_i(t)\to\infty$ and $\lim_{t\to\infty}\dot{q}_i(t)\to\infty$, and hence $\lim_{t\to\infty}\dot{w}_1(x_1,t)\to\infty$. This implies the kinetic energy $E_k$ of the system approaches infinity, which contradicts the fact the $V_i\ (i=1,2,3)$ is actually bounded. Therefore, $D_1^i$ must be zero. Consequently, the solution (16) approaches zero as time approaches infinity.

In summary, $w_1(x_1,t)=0$ provided that the system motion is in the largest invariant set in the set $\dot{V}_i=0\ (i=1,2,3)$. Moreover, recalling that we already have $\theta_1=\theta_{d1}$, we further conclude that if the system motion is in the largest invariant set in the set $\dot{V}_i=0\ (i=1,2,3)$, the first link must stop in the final position described by $\theta_1=\theta_{d1}$ and $w_1(x_1,t)=0$. Thus, the local frame $O_2X_2Y_2$ is actually static with respect to the inertia frame $O_1X_1Y_1$. This allows us to take $O_2X_2Y_2$ as the inertia frame in which link 2 is to be considered. Then we have the following PDEs of link 2:

$$c_{e2}w_2''(0,t)-k_{p2}(\theta_2-\theta_{d2})=0 \tag{18}$$

$$\rho_{L2}\ddot{w}_2(x_2,t)=-c_{e2}w_2''''(x_2,t),\qquad 0\leq x_2\leq L_2. \tag{19}$$

Moreover, from the above conclusions, a set of boundary conditions similar to (12) and (15) also exist for (19), i.e.,

$$w_2(0,t)=0$$
$$w_2'(0,t)=0$$
$$w_2''(0,t)=0$$
$$w_2''(L_2,t)=0.$$

Thus, carrying out similar analysis for link 2 leads to the conclusion that link 2 must stop at its final position described by $\theta_2=\theta_{d2}$ and $w_2(x_2,t)=0$ provided that the system motion is in the largest invariant set in the set $\dot{V}_i=0\ (i=1,2,3)$. This implies the local frame $O_3X_3Y_3$ can be considered as the inertia frame for link 3. Now it is easy to see that repeating the same procedure until link $N$ finally leads to the fact that if the system motion is in the largest invariant set in the set $\dot{V}_i=0\ (i=1,2,3)$, then all links must stop at their final positions, i.e., $\theta_i=\theta_{di}$ and $w_i(x_i,t)=0\ (i=1,2,\ldots,N)$.

Now, let us consider the case when the right-hand side of either (13) or (14) is a nonzero constant as discussed. If this is true, then from $w_1(x_1,t)=\Psi(x_1)Q(t)$, $Q(t)$ and hence, $w_1(x_1,t)$ must be constant. This means that the first link is static, which implies that the right side of both (13) and (14) must equal the same nonzero constant (from the moment balance of a static bending beam). Subsequently, frame $O_2X_2Y_2$ can be taken as the inertia frame for link 2. Because the base bending moment of link 2 equals the tip bending moment of link 1 (note the condition $\dot{V}_i=0$), the base bending moment of link 2 must be the same constant. This, by assuming $w_2(x_2,t)=\Psi(x_2)Q(t)$, implies link 2 is also static. Repeating the same procedures for all links leads to a static bending $N$-link robot. Then, from the moment balance of the static robot, the base bending moment of link 1 should be equal to the tip bending moment of link $N$. Since the free tip of link $N$ is loaded with a concentrated mass, the tip bending moment is zero. Therefor, either the base bending moment of link 1 or its tip bending moment must be zero.

Now, invoking the truncation assumption, the elastic deflection of each link is assumed to be described by a finite number of flexible modes, and subsequently the system is of only finite dimensions. For this truncated system, because it has been proven already that the largest invariant set in the set $\dot{V}_i=0\ (i=1,2,3)$ is the final equilibrium position, the asymptotic stability directly follows the LaSalle's theorem.

TABLE I
SYSTEM PARAMETERS

| | Link 1 | Link 2 |
|---|---|---|
| Beam length(m) | 1.0 | 0.8 |
| Beam width(m) | 0.01 | 0.01 |
| Sensor thickness(m) | 0.0004 | 0.0004 |
| Actuator thickness(m) | 0.0008 | 0.0008 |
| Beam linear density(Kg/m) | 0.1 | 0.1 |
| Beam stiffness(N/$m^2$) | $6\times10^8$ | $6\times10^8$ |
| PM length(m) | 0.01 | 0.01 |
| PM density(Kg/$m^3$) | 1800 | 1800 |
| PM stiffness(N/$m^2$) | $8\times10^6$ | $8\times10^6$ |
| impermittivity(m/F) | $4\times10^{14}$ | $4\times10^{14}$ |
| coupling parameter(v/m) | $5\times10^{11}$ | $5\times10^{11}$ |
| Hub inertia(Kg/$m^2$) | 3.0 | 1.5 |
| Payload(Kg) | 0.1 | 0.05 |

## IV. SIMULATION TESTS

Numerical simulations are carried out on a two-link smart materials robot moving in the horizontal plane. The plant is simulated by an FEM model in which each link is divided into four elements with same length, system parameters are given in Table I where PM refers to piezoelectric material. A fourth-order Runge–Kutta program with adaptive step size is used to numerically solve the differential equations. In simulation, $\theta_{d1}=30^\circ$ and $\theta_{d2}=20^\circ$, while $\theta_1(0)=0^\circ$ and $\theta_2(0)=0^\circ$. The two lowest natural frequencies of the system at $\theta_2=20^\circ$ are approximated as $f_1=4.2$ Hz and $f_2=13.4$ Hz, [16]. The robot is assumed to be initially at rest without any deformation.

Following the discussion in [9], the feedback gains are chosen as $K_p=[21.6,14.0]$, $K_v=[17.3,9.3]$, and $k_{1i}=6000$ for EBRC 1 and $k_{2i}=2000$ for EBRC 2.

DMFC and CMFC controllers used for simulations are given by

*DMFC:*

$$\mathbf{u}_i=\begin{bmatrix}\tau_i\\ \mathbf{v}_i\end{bmatrix}=\begin{bmatrix}-k_{pi}[\theta_i(t)-\theta_{di}]-k_{vi}\dot{\theta}_i(t)\\ -\mathbf{K}_{vsi}\mathbf{I}_i(t)\end{bmatrix}.$$

*CMFC 1:*

$$\mathbf{u}_i=\begin{bmatrix}\tau_i\\ \\ \mathbf{v}_i\end{bmatrix}=\begin{bmatrix}-k_{pi}[\theta_i(t)-\theta_{di}]-k_{vi}\dot{\theta}_i(t)-\sum_{j=1}^{2}\\ k_{\theta j}w_j(L_j,t)\int_0^t\dot{\theta}_i(s)w_j(L_j,s)ds\\ -\mathbf{K}_{vsi}\mathbf{I}_i(t)\end{bmatrix}$$

where $k_{\theta j}=Y_{\theta j}^2$, and

$$\dot{Y}_{\theta j}(t)=\alpha_{\theta j}Y_{\theta j}\dot{\theta}_j w_j(L_j,t)\int_0^t\dot{\theta}_i w_j(L_j,s)ds-\sigma_{\theta j}Y_{\theta j}(t).$$

*CMFC 2:*

$$\mathbf{u}_i=\begin{bmatrix}\tau_i\\ \\ \mathbf{v}_i\end{bmatrix}=\begin{bmatrix}-k_{pi}[\theta_i(t)-\theta_{di}]-k_{vi}\dot{\theta}_i(t)-\sum_{j=1}^{2}\\ k_{\theta j}w_j''(0,t)\int_0^t\dot{\theta}_i(s)w_j''(0,s)ds\\ -\mathbf{K}_{vsi}\mathbf{I}_i(t)\end{bmatrix}$$

where $k_{\theta j}=Y_{\theta j}^2$, and

$$\dot{Y}_{\theta j}(t)=\alpha_{\theta j}Y_{\theta j}\dot{\theta}_i w_j''(0,t)\int_0^t\dot{\theta}_i w_j''(0,s)ds-\sigma_{\theta j}Y_{\theta j}(t).$$

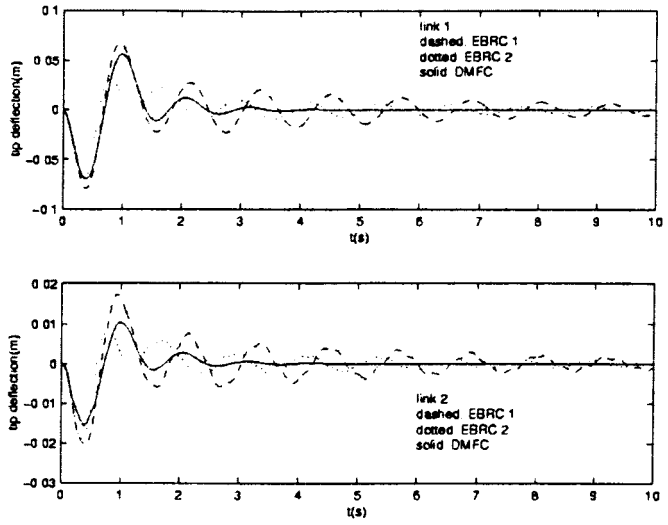


Fig. 2. Tip deflections under *EBRC* and *DMFC*.

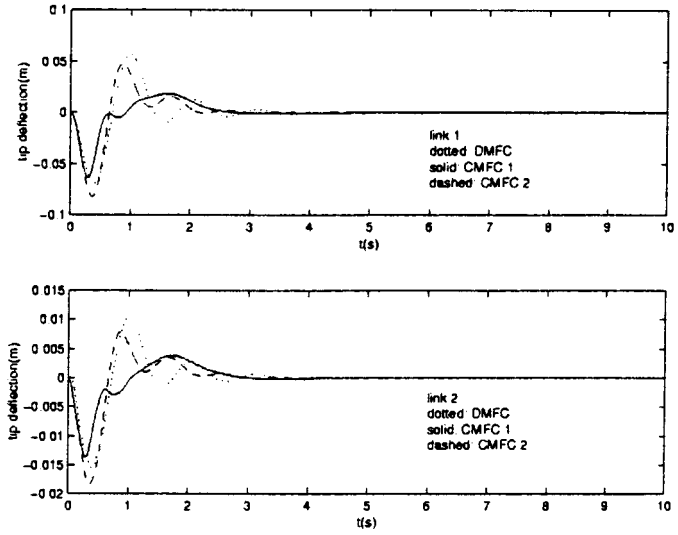


Fig. 3. Tip deflections under *DMFC* and *CMFC*.

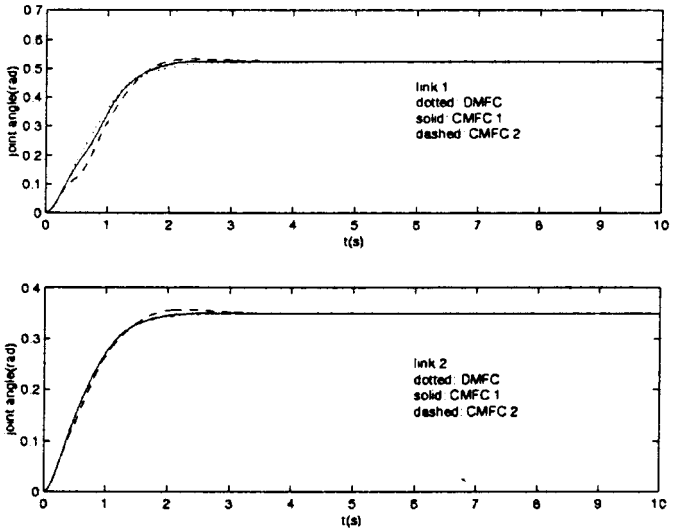


Fig. 4. Joint angle under *DMFC* and *CMFC*.

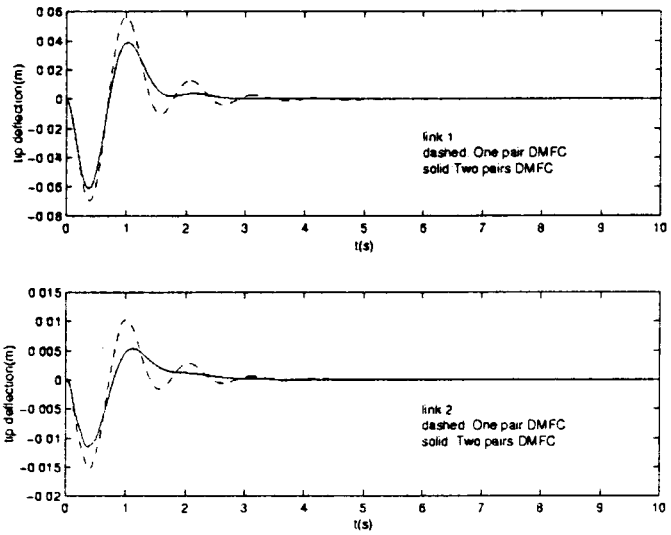


Fig. 5. Tip deflections of *DMFC*.

### *A. Using One Pair of Smart Sensor and Actuator*

First, let us consider the case where only one pair of smart sensor and actuator is used for each link. The pair of piezoelectric patches are located at $x_i = 0.1L_i$ of each link with $L_i$ being the full length of each link.

Fig. 2 shows the deflection of DMFC with large enough feedback gain $k_{\rm vsi} = 6 \times 10^6$ due to the low authority of the piezoelectric material in comparison with the relatively good EBRC. It can be seen that DMFC is quite effective in residual vibration suppression in comparison to EBRC. Though the transient responses are about the same, there is a big difference at steady state. While there is no residual vibration at steady state for DMFC, there exists residual vibration of small magnitude for EBRC. Fig. 3 shows the tip deflection of DMFC and CMFC's. The parameters are chosen as $\alpha_{\theta j} = 1000$, $\sigma_{\theta j} = 0.1$, and $k_{\theta j}(0) = 1000$. It can be seen that CMFC's give a quicker response with small overshoot and less oscillation. Fig. 4 shows that all controllers can drive the system to the desired joint angular position.

### *B. Using Multipairs of Smart Sensors and Actuators*

It is interesting to investigate the control performance when additional pairs of smart sensors and actuators are used. Assumed that for each link, there are two pairs of smart sensors and actuators distributed at $x_{i1} = 0.1L_i$ and $x_{i2} = 0.1L_i + h_i$ with $h_i$ the element length.

Fig. 5 shows the tip deflections of the two links under DMFC with one pair, two pairs, and four pairs of piezoelectric actuators and sensors. For comparison, the feedback gains are still chosen as $k_{\rm vsi} = 6 \times 10^6$. It is clear that the two-pair case can suppress residue vibration quickly and smoothly than the one pair case. Fig. 6 shows the tip deflection of the individual link for one and two pair cases. The residual vibration suppression improves as the numbers of pairs are activated as shown in Fig. 6.

Through the simulation study, we have shown the effectiveness of both DMFC and CMFC controllers, despite its control low authority in control action. For more precise control performance, more pairs of piezoelectric actuators and sensors can be bonded. It should be pointed out that DMFC and CMFC can be applied according to different system configurations, and other kinds of feedbacks and/or other kinds of combinations of feedbacks can also be considered depending on the available sensor facilities, since the controllers actually allow a great deal of freedoms of engineering implementation and controller design.

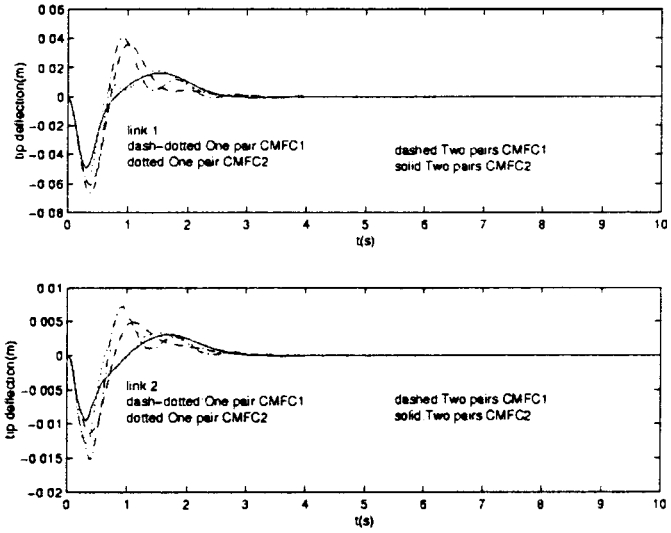


Fig. 6. Tip deflections of *CMFC*.

## V. Conclusion

In this paper, two kinds of model-free controllers for multilink flexible smart materials robot were presented. Theoretical proofs have shown that both of them can stabilize the closed-loop system, and the controllers are independent of system parameters, hence, possess stability robustness to parameter variations. The effectiveness of the proposed controllers has been proved by numerical simulations.

## References

[1] R. H. Cannon Jr and E. Schmitz, "Initial experiments on the end-point control of a flexible robot," *Int. J. Robot. Res.*, vol. 3, no. 3, pp. 62–75, 1984.

[2] A. Arakawa, T. Fukuda, and F. Hara, "$H_\infty$ control of a flexible robotics arm (effect of parameter uncertainties on stability)," in *Proc. 1991 IROS*, pp. 959–964.

[3] Y. Sakawa, F. Matsuno, and S. Fukushima, "Modeling and feedback control of a flexible arm," *J. Robot. Syst.*, vol. 2, no. 4, pp. 453–472, 1985.

[4] J. H. Yang, F. L. Lian, and L. C. Fu, "Nonlinear adaptive control for flexible-link manipulators," *IEEE Trans. Robot. Automat.*, vol. 13, pp. 140–146, Feb. 1997.

[5] B. Siciliano and W. J. Book, "A singular perturbation approach to control of lightweight flexible manipulator," *Int. J. Robot. Res.*, vol. 7, no. 4, pp. 79–89, 1988.

[6] Z. H. Luo, "Direct strain feedback control of flexible robot arm: New theoretical and experimental results," *IEEE Trans. Automat. Contr.*, vol. 38, pp. 1610–1622, Nov. 1993.

[7] G. Zhu and S. S. Ge, "A quasitracking approach for finite-time control of a mass-beam system," *Automatica*, vol. 34, no. 7, pp. 881–888, 1998.

[8] S. S. Ge, T. H. Lee, and G. Zhu, "Asymptotically stable end-point regulation of a flexible SCARA/Cartesian robot," *IEEE/ASME Trans. Mechatron.*, vol. 3, pp. 138–144, June 1998.

[9] ——, "Energy-based robust controller design for multi-link flexible robots," *Mechatronics*, vol. 6, no. 7, pp. 779–798, 1996.

[10] E. F. Crawley and J. Luis, "Use of piezoelectric actuators as elements of intelligent structures," *AIAA J.*, vol. 25, no. 10, pp. 1373–1385, 1987.

[11] V. K. Varadan, S. Y. Hong, and V. V. Varadan, "Piezoelectric sensors and actuators for active vibration damping using digital control," in *Proc. IEEE Ultrasonics Symp.*, Honolulu, HI, 1990, pp. 1211–1214.

[12] F. Khorrami, I. Zeinoun, and E. Tome, "Experimental result on active control of flexible-link manipulators with embedded piezoceramics," in *Proc. 1993 IEEE Int. Conf. Robotics and Automation*, vol. 3, pp. 222–227.

[13] S. S. Ge, T. H. Lee, J. Q. Gong, and Z. P. Wang, "Model-free controller design for a single-link flexible smart materials robot," *Int. J. Control*, vol. 73, no. 6, pp. 531–544, 2000.

[14] C. C. Won, "Piezoelectric transformer," *J. Guid. Control Dyn.*, vol. 18, no. 1, pp. 96–101, 1995.

[15] L. Meirovitch, *Elements of Vibration Analysis*, 2nd ed. New York: McGraw-Hill, 1986.

[16] Robert and D. Blevins, *Formulas for Natural Frequency and Mode Shape*. New York: Van Nostrand, 1979.

# End-Point Sensing and State Observation of a Flexible-Link Robot

Y. F. Li and X. B. Chen

***Abstract*—This paper presents an end-point sensor system and the development of an observer to reconstruct the states of a flexible-link robot. The sensor system includes a tip displacement sensor and an accelerometer. Based on the assumed-models method, an observer is developed using the Kalman filtering algorithm. Experimental results are given to demonstrate the effectiveness of the observer.**

***Index Terms*—End-point sensing, flexible link, Kalman filter, observer, robot.**

## I. Introduction

The control of flexible-link robots is difficult due to the presence of the flexible modes [1]. In particular, the control of the endpoint trajectory to achieve a desired position and velocity is a challenging task. To achieve a desired control performance, the knowledge of the state variables of the endpoint is often needed. For a rigid link, the tip position can be determined by using measurements from the shaft encoder. For a flexible link, however, this problem becomes rather complicated due to the presence of the structural deflection of the link. To measure the tip deflection, different attempts have been made by researchers over the past years. One is to use strain gauges [2] by which local deformation information can be obtained. However, the deflection at the tip needs to be derived from the measurements taken from several locations along the link, which tends to make the result inaccurate. Obviously, a method that can directly measure the structural deflection at the tip is desirable. Optical measurement systems which used lasers and position-sensitive devices (PSD) were explored for this purpose [3], [4]. Vision systems were also used to measure the structural deflections of flexible links [5], [6]. A major problem with this method is the time-consuming computation needed for the visual processing in real-time applications. Besides the tip position, information on the velocity and acceleration at the tip is also useful for the control of flexible-link robots. The endpoint acceleration can be measured using an accelerometer mounted on the tip. The tip velocity, however, has proved difficult to measure by using hardware at the tip.

Due to such difficulties in measuring the full states of a flexible-link robot, a state observer is desired. There are a few observers developed for this purpose in the literature. Using the measurements of the joint

Manuscript received November 13, 2000; revised May 15, 2001. This work was supported by the Research Grants Council of Hong Kong under Grant CityU1137/97E (9040309). Recommended by Technical Editor M. Meng.

Y. F. Li is with the Department of Manufacturing Engineering and Engineering Management, City University of Hong Kong, Kowloon, Hong Kong (e-mail: meyfli@cityu.edu.hk).

X. B. Chen is with the Department of Mechanical Engineering, University of Saskatchewan, Saskatoon, SK S7N 5A9 Canada (e-mail: xbc719@mail.usask.ca).

Publisher Item Identifier S 1083-4435(01)08148-0.